# SOME NUMERICAL SOLUTIONS OF UNSTEADY FREE SURFACE WAVE PROBLEMS USING THE LAGRANGIAN DESCRIPTION OF THE FLOW

Christopher Brennen
California Institute of Technology

## INTRODUCTION

Until very recently numerical solutions of unsteady, free surface flows invariably employed the Eulerian description of the motions. Perhaps the most widely used of these has been the marker and cell (MAC) technique developed by Fromm and Harlow (1963) and further refined by many others. In such a formulation the most difficult problem arises in attempting to reconcile the initially unknown shape and position of the free surface with a finite difference scheme and the necessity of determining derivatives at that surface (in a similar fashion few solutions exist with curved or irregular boundaries). But this difficulty can be surmounted by solving in a parametric plane in which the position and shape of the free surface are known in advance; such mappings have been successfully employed in steady flows (eg. Brennen (1969)). Whilst there are other possibilities (see John (1953), Brennen and Whitney (1970)) the Lagrangian description in its general form involves just such a parametric plane. The present paper describes briefly a numerical method for the solution of the Lagrangian equations of motion for the inviscid, planar flow of a homogeneous or inhomogeneous fluid, taking full advantage of the flexibility of choice of the Lagrangian coordinates (a,b). More details and other results can be found in Brennen and Whitney (1970). Very recently Hirt, Cook and Butler (1970) published details of a method which solves the Eulerian equations of motion in a fashion similar to the MAC technique but uses a Lagrangian tagging space.

## BASIC EQUATIONS

The general inviscid dynamical equations of planar motion in Lagrangian form are (Lamb (1932)):

$$(X_{tt} - F)\begin{Bmatrix} X_a \\ X_b \end{Bmatrix} + (Y_{tt} - G)\begin{Bmatrix} Y_a \\ Y_b \end{Bmatrix} + \frac{1}{\rho}\begin{Bmatrix} P_a \\ P_b \end{Bmatrix} = 0 \qquad (1)$$

where $X,Y$ are the cartesian coordinates of a fluid particle at time $t$, $F,G$ are the components of extraneous force acting on it, $P$ is pressure, $\rho$ the density and $(a,b)$, the Lagrangian coordinates, are any two quantities which serve to identify the particle and vary continuously from one particle to the next. Subscripts $a,b,t$ denote differentiation. The equation of continuity is simply

$$\rho\, \partial(X,Y)/\partial(a,b) = \text{independent of time, } t \qquad (2)$$

If $F,G$ have a potential and $\rho$, if not uniform, is a function only of $P$ then from (1)

$$\frac{\partial}{\partial t}(U_a X_b - U_b X_a + V_a Y_b - V_b Y_a) = -\frac{\partial \Gamma}{\partial t} = 0 \qquad (3)$$

where $U,V$ are the velocities $X_t, Y_t$. It is easily shown that $\Gamma$ is the vorticity multiplied by the Jacobian $(X_a Y_b - X_b Y_a)$ and can be calculated from the initial conditions. By introducing the vectors $Z = X + iY$, $W = U - iV$ the equations of motion, (3), and continuity ((2) differentiated w.r.t. $t$) conveniently combine to

$$Z_a W_b - Z_b W_a = \Gamma(a,b) \qquad (4)$$

In the case of an inhomogeneous fluid with no density diffusion (i.e., $\rho = \rho(a,b)$) equation (3) must be modified and the resulting equivalent of (4) is:

$$Z_a W_b - Z_b W_a = \left[\Gamma(a,b)\right]_{t=t_o} - \frac{1}{\rho}\int_{t_o}^{t} (X_{tt} - F)(\rho_b X_a - \rho_a X_b) + (Y_{tt} - G)(\rho_b Y_a - \rho_a Y_b)\, dt \qquad (5)$$

The integral represents the vorticity generated by the density gradients.

## NUMERICAL METHOD FOR SOLUTION

The following method was designed to numerically solve the equations (4) or (5) of the preceding section. It was an implicit scheme with central differencing over a series of stations in time, t, distinguished by the integer superscript p. The values $Z^{p+1}$ are determined by solving for the velocities, $Z_t = \overline{W}$, at midway stations, $p+\frac{1}{2}$, and then employing the numerical approximation:

$$Z^{p+1} = Z^p + \tau \overline{W}^{p+\frac{1}{2}} \quad (\text{error order } \tau^3 Z_{ttt}) \tag{6}$$

where $\tau$ is the time interval dividing stations $p+1$ and $p$.

The method is necessarily restricted to a finite body of fluid, S; this might, however, be part of a larger or infinite mass provided an "outer" approximate solution of sufficient accuracy was available to provide matching conditions at the interface. Then S need not be fixed in time. In a great many cases it is possible and convenient to choose S to be rectangular in the (a,b) plane. This rectangle (ABCD, figure 1) is divided into a set of elemental rectangles or 'cells' the motion

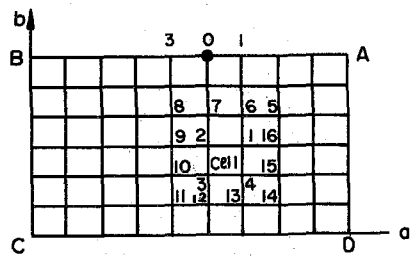


FIGURE 1

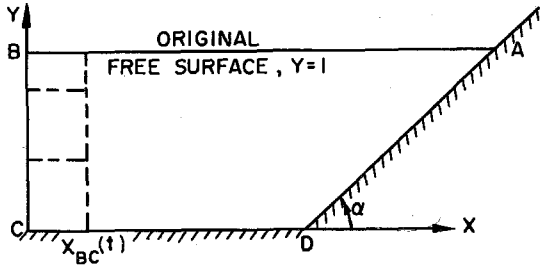


FIGURE 2

of each of which is to be followed by determining the Z values at all the nodes.

Equation (4) or (5) is discretized by integrating over the area of a general cell in the (a,b) plane using Taylor expansions about the center of that cell. This produces the first and second order terms of the Cell Equation, (7). The cell circulation $\Gamma_c$ is calculated from the initial conditions at $t = t_o$. Subscripts refer to values at particular nodes surrounding the general cell as shown in figure 1.

$$\begin{aligned}
&(Z_2 - Z_4)(W_1 - W_3) - (Z_1 - Z_3)(W_2 - W_4) - 2\Gamma_c && \text{First Order}\\
&+ \tfrac{1}{12}\{(W_{16} + W_9 - W_1 - W_2)(Z_1 - Z_2) - (W_{15} + W_{10} - W_3 - W_4)(Z_4 - Z_3) && \text{Second Order Term}\\
&\quad + (W_7 + W_{12} - W_2 - W_3)(Z_2 - Z_3) - (W_6 + W_{13} - W_1 - W_4)(Z_1 - Z_4)\} && \text{if required}\\
&+ i\tau\{(U_1 - U_3)(V_2 - V_4) - (U_2 - U_4)(V_1 - V_3)\} + 2i(A^p - A^o)/\tau && \text{Continuity Corrections}\\
&+ \theta^{p+\frac{1}{2}} && \text{Inhomogeneous term (see later)}\\
&= 0 = R_I + iR_c = R, \text{ The Cell Residual} && (7)
\end{aligned}$$

Since the values referred to are $Z^p$ and $\{W,U,V\}^{p+\frac{1}{2}}$ the first of the continuity corrections is required to allow for this fact (see Brennen and Whitney (1970)). The second prevents accumulation of error over many time steps, A being the area of the cell. Then the equations (7), one for each cell, are to be solved for $W^{p+\frac{1}{2}}$, $Z^p$ being known. Boundary conditions most often take the form of a relation connecting $U^{p+\frac{1}{2}}$ and $V^{p+\frac{1}{2}}$. Solid boundaries will be prescribed in the form $F(X,Y,t) = 0$ which leads to the relation $F(X^p + \tau U^{p+\frac{1}{2}}, Y^p + \tau V^{p+\frac{1}{2}}, t) = 0$. Dynamic free surface conditions are simply given through the equations of motion, (1). Thus if the line AB, figure 1 is a free surface, equation (1) leads to the following first order numerical constant pressure condition at a node such as 0, figure 1:

$$(X_1 - X_3)^p (U_o^{p+\frac{1}{2}} - U_o^{p-\frac{1}{2}}) + (Y_1 - Y_3)^p (V_o^{p+\frac{1}{2}} - V_o^{p-\frac{1}{2}} + \tau g) = 0 \tag{8}$$

where the only extraneous force is that due to gravity, g, in the negative Y direction. Again (8) connects $U_o^{p+\frac{1}{2}}$ to $V_o^{p+\frac{1}{2}}$, all other quantities being known.

Solution was effected by the iterative method of successive relaxation of the cells according to

$$\Delta W_1 = -\Delta W_3 = \omega i R(\overline{Z_1 - Z_3})/8A \; ; \; \Delta W_2 = -\Delta W_4 = \omega i R(\overline{Z_2 - Z_4})/8A \qquad (9)$$

$\omega$ being an overrelaxation factor. These incremental velocity changes have a simple physical interpretation. They contain two components, one of pure stretching and one of pure rotation of the cell which respectively dissipate the continuity and circulation components of the cell residual, R. After one sweep over all cells, the boundary conditions were imposed and the process repeated to convergence.

If the fluid is inhomogeneous then further advantage can be taken of the flexibility in the choice of (a,b) by choosing $Z^o(a,b)$ so that $\rho$ is some simple analytic function of a and b. For example, if $\rho$ is constant on the free surface, AB (figure 1) and along the bed, CD, an appropriate choice of $\rho$ may be $\rho = \rho_{CD}(1+\delta b)$.

Then integration over the cell area yields the following expression for $\Theta^{p+\frac{1}{2}}$ in equation (7) corresponding to the integral term in equation (5):

$$\theta^{p+\frac{1}{2}}_{1234} = \theta^{p-\frac{1}{2}}_{1234} - \frac{1}{4}\ln(1-\mu)\ \mathrm{Real}\left[\sum_{N=1}^{4}\left\{(Z_1 - Z_2 - Z_3 + Z_4)^p (W_N^{p+\frac{1}{2}} - W_N^{p-\frac{1}{2}} - i\tau g)\right\}\right]$$

$$+\left\{1+\left(\frac{1}{\mu}-\frac{1}{2}\right)\ln(1-\mu)\right\}\left[\mathrm{Real}\left\{\sum_{N=1}^{2}(Z_{2N-1}-Z_{2N})^p (W_{2N-1}^{p+\frac{1}{2}} + W_{2N}^{p+\frac{1}{2}} - W_{2N-1}^{p-\frac{1}{2}} - W_{2N}^{p-\frac{1}{2}} - 2i\tau g)\right\}\right]$$

where $\mu = \delta\Delta b/(1+\delta b_{34})$, $b_{34}$ being the value of b on the side 34 of the cell and $\Delta b$ the b difference across each and every cell.

More detail, including error and stability analyses are contained in Brennen and Whitney (1970).

## SAMPLE SOLUTIONS

The feasibility and potential of the method have been tested in a variety of examples of free surface flow. In two simple cases of wave generation, one by vertical wall movement (wavemaker) and one by bed movement (tsunami model) the numerical results agreed satisfactorily with Lagrangian linearized solutions at small amplitudes and showed the divergences expected from non-linear effects as the wave height increased (Brennen and Whitney (1970)). Solutions involving the interactions of waves thus generated with various boundary geometries such as a beach or a shelf have also been obtained. Only two examples can be presented in the limited space available here. In both cases the results are non-dimensionalized using the original water depth, h, as typical length and $(h/g)^{\frac{1}{2}}$ as typical time.

In the first example fluid is originally at rest in the container ABCD, figure 2. The side BC then moves inward according to $X_{BC} = M\sin^2(\pi t/2T)$ in the interval $0 < t < T$ thereafter remaining at $X_{BC} = M$. This creates a wave which travels across the container and reacts with the beach. The positions of the free surface at a selected number of time stations are shown in figures 3 and 4; in the former $M = 0.30$, $T = 6\tau$, $\tau = 0.571$, $\alpha = 27^o$, in the latter the values are 0.6, $8\tau$, 0.571 and $18^o$ respectively. The reaction with the beach is similar in both cases. Prior to maximum run-up the motions are fairly smooth. However the downwash and its associated fluid motions rapidly become rather violent. Positions $t/\tau = 21, 22$ of figure 3 and $t/\tau = 23, 25$ of figure 4 suggest that this causes 'downwash wave breaking'. By the last times shown the cells have become very distorted and the mesh points excessively widely spaced to allow further progress.

In figure 5, the fluid is originally at rest in a container, half of which is shown as ABCD. In this position it has a vertical, linear density gradient, $\rho = \rho_o(1+\delta Y)$, $\delta$ being negative. Symmetric with the center line, BC, a portion of the bed then begins to oscillate sinusoidally in time as shown in figure 6, the shape of the bed disturbance also being sinusoidal. With the same excitor frequency ($\omega = 0.125$) solutions were obtained for various $\delta$ with a view to observing

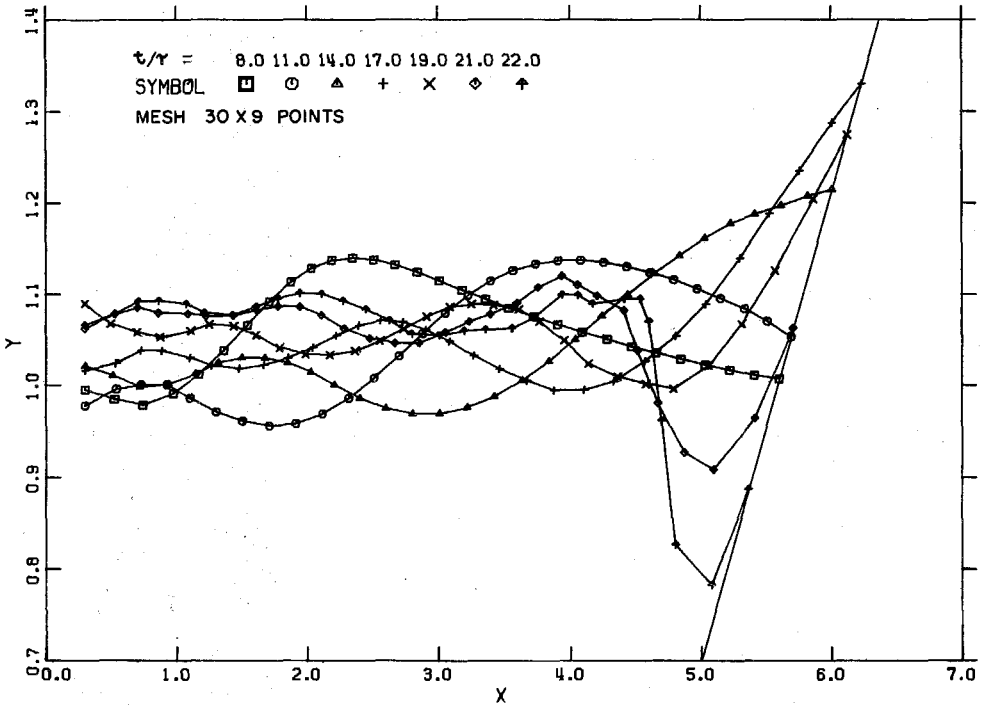


FIGURE 3

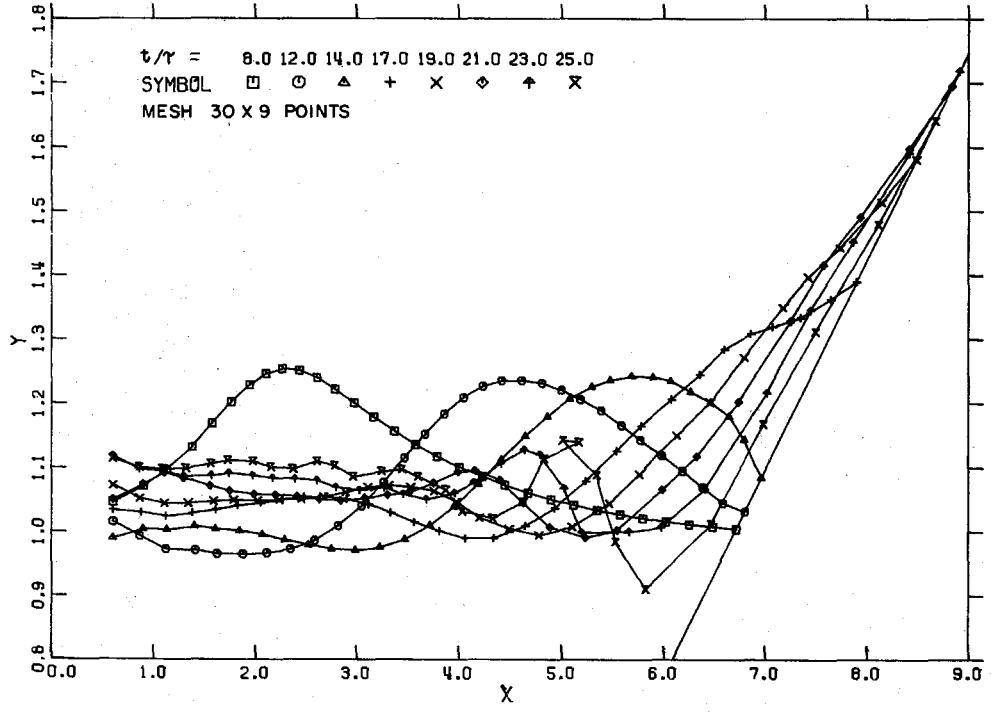


FIGURE 4

internal waves when the bed Väisälä frequency $N_o = (-g\delta)^{\frac{1}{2}}$ exceeded the excitor frequency. In figures 7 and 8, the configuration of three originally horizontal lines (at Y = 0.667, 0.883 and 1.00) at the half cycle (□), 3/4 cycle (○), full cycle (△) and 1 1/4 cycle (+) time stations are shown for the cases $N_o/\omega = 0.8$ and 1.2. The profiles in the former case differ only slightly from the homogeneous

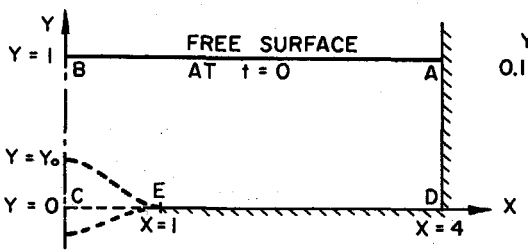


FIGURE 5

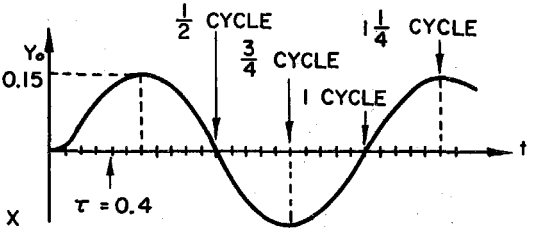


FIGURE 6

results with $N_o/\omega = 0$. Clearly the latter case is very different. Internal wave troughs can be observed in the 3/4 cycle profiles and peaks in the 1 1/4 cycle profiles. These peaks and troughs lie close to the line FF, drawn through the origin at an angle of $\tan^{-1}[(N_o/\omega)^2 - 1]^{\frac{1}{2}}$ to the horizontal (GG is drawn through the end of the excitor, E). This is the slope of the characteristic predicted by linearized theory (Wu (1966)) for a point disturbance. Positions of the cells after one cycle are shown in figure 9 with the lines of zero vorticity (·····) and the lines FF, GG superimposed. Also included is a line, HH, drawn so that its slope is everywhere $[(N/\omega)^2 - 1]^{\frac{1}{2}}$, N being the Väisälä frequency at each particular vertical

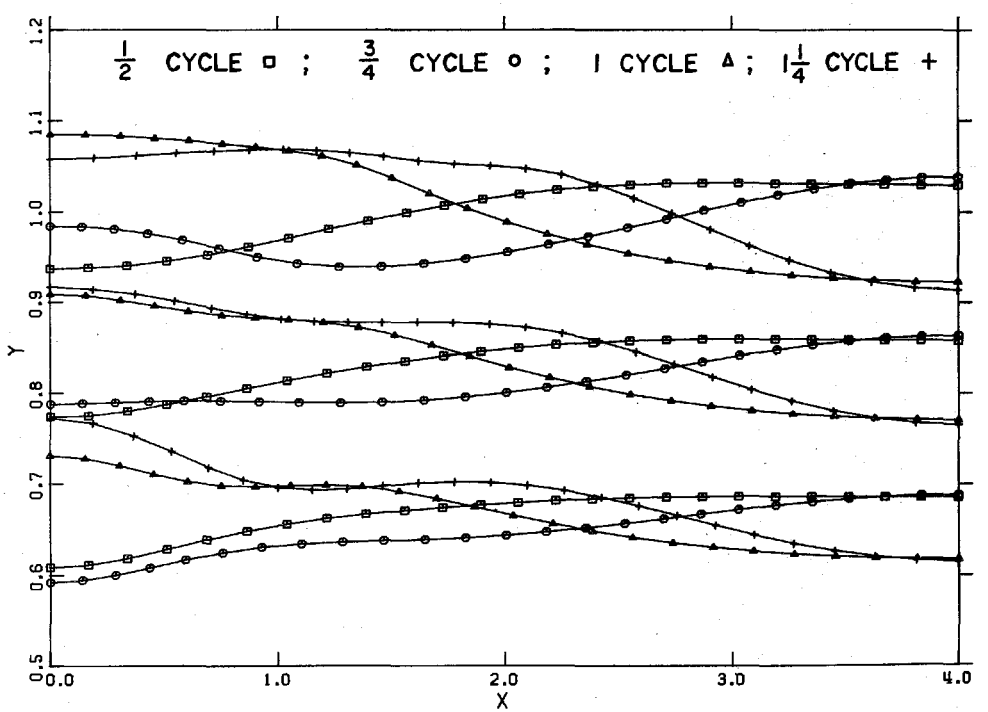


FIGURE 7

elevation ($N^2 = -g\delta/(1 + \delta(Y)_{t=0})$).

Other types of examples which have been only briefly investigated thus far are: the matching with a semi-infinite region in which some analytic solution is used; the inclusion of surface tension; extension to three dimensions. It is hoped to present such results in the near future.

This work was partially sponsored by the National Science Foundation under grant GK 2370 and by the Office of Naval Research. The author deeply appreciates the considerate help given by Professor T. Y. Wu and Dr. A. K. Whitney.

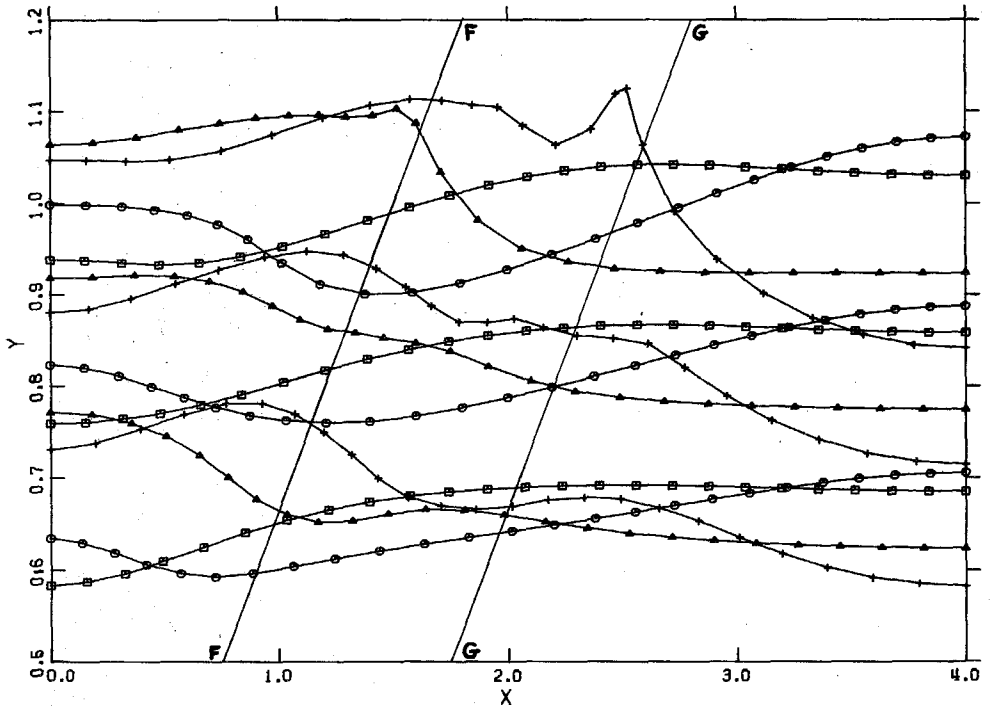


FIGURE 8

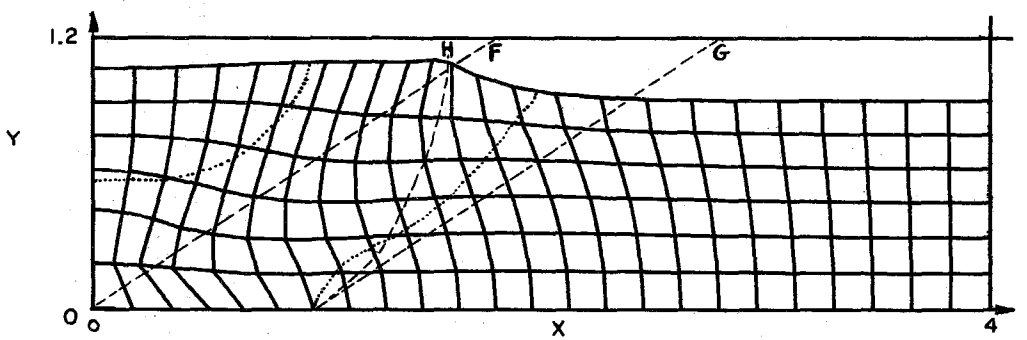


FIGURE 9

## REFERENCES

Brennen, C. J. Fluid Mech., 37, 4 (1969).
Brennen, C. and Whitney, A. K. 8th O.N.R. Symposium on Naval Hydrodynamics, Aug. 1970.
Fromm, J. E. and Harlow, F. H. Physics of Fluids, 6 (1963).
Hirt, C. W., Cook, J. L. and Butler, T. D. J. Computational Physics, 5 (1970).
John, F. Comm. Pure and Appl. Math, 6 (1953).
Wu, T. Y. 6th O.N.R. Symposium on Naval Hydrodynamics, Sept. 1966.